Gas Processing Journal

Vol. 8, No. 1, 2020, pp. 69-82
http://gpj.ui.ac.ir

DOI: http://dx.doi.org/10.22108/gpj.2020.120776.1075

Numerical Investigation on Efficiency of Inertial Sand Separators of a Gas Turbine

Reza Shahraki Shahdabadi [1], Pouria Lotfi [2], Ghodrat Ghassabi [3*]

[1,2,3] Department of Mechanical Engineering, Bozorgmehr University of Qaenat, Qaen, Iran

Received: 2019-12-28 Revised: 2020-04-09 Accepted: 2020-04-20

Abstract: Gas turbine inlet air is filtered in multiple steps. First, the filtration step is used for removing the big things. Then, Sand and dust are removed using the inertial sand separators. Sand separators filtration system is composed of 30 rows of the inertial sand separators on 5 floors. In this paper, one floor of the inertial sand separators filtration system of Shahid Kave power plant has been simulated using Ansys Fluent 16. A computational server with 20 processing cores and RAM of 120 GB was used to carry out the calculations. The velocity and pressure fields have been studied and the effect of density and diameter of particles on inertial sand separators efficiency are investigated. Particle diameter and density are varied between 0.1 to 100 micrometer and 500 to 2000 kg/m^3 respectively. The result shows that the collection efficiency of the inertial sand separators was reduced by increasing the particle diameter. However, the collection efficiency of the inertial sand separators was improved by increasing the particle density. Also, a few particles are collected by inertial sand separators, so that collection efficiency is less than 1%. Therefore, this system is inefficient and not cost-effective and elimination of the system fans could reduce the energy consumption of the gas power plant around 360 kW.

keywords: Particles separation, Turbulence flow, Discrete phase, Collection Efficiency

1. Introduction

The dramatic reduction in energy resources in recent decades has highlighted the optimum use of energy as a predominant issue, particularly electrical energy that has played an important role in the world's industry. Also, gas turbine power plants are one of the most central resources of electrical energy production. Since the working fluid of gas turbine is air and they operate within an open cycle, it is vital to filter the compressor intake air from particles and objects to avoid any damage to expensive equipment (e.g. compressor and turbine blades) and prevent from inappropriate combustion (leading to efficiency reduction). Dust sources in the intake air are highly diverse. One of the most crucial pollution sources is microscopic sand grains with the diameter exceeding $0.3\mu m$ and being transferred through desert regions.

There are various approaches to particle separation and air remediation. One of the key particle separation methods is founded on inertia. It is intended in this method to subject fluid flow to gravity so that particles get separated due to their weight force. Numerous studies have been conducted in this field.

Amini et al. (Amini, Lee, & Di Carlo, 2014) investigated particle separation by the aid of inertia in helical channels, concluding that lift and drag forces along with centrifugal force (due to the helical shape of the channel) played an effective role in the particle separation process.

One of the most significant inertia-based equipment for separation is cyclone particle separator. The separation process of air particles in cyclone is performed in an intensive gravity field which is artificially generated. The main function of cyclones is to separate dust from the gas flow. Safikhani et al. (Safikhani, 2016) presented a paper on the performance of a cyclone separator device, as well as its design. They showed that the pressure drop decreased by increasing the clearance between the vortex finder and vortex limiter, increasing the length of the vortex finder, and enlarging the diameter of the

* Corresponding Author.
Authors' Email Address: [1] R. Shahraki Shahdabadi (reza3669855@gmail.com), [2] P. Lotfi (pouria.lotfi74@gmail.com), [3] Gh. Ghassabi (ghodrat.ghassabi@buqaen.ac.ir)
ISSN (Online): 2345-4172, ISSN (Print): 2322-3251

vortex limiter. Khazaee (Khazaee, 2017) studied numerically effects of number and shape of a cyclone on particle separation. The results show that collection efficiency increases with increasing the number of inlets. Also, their results show that the shape of inlets has a significant effect on cyclone performance. Kumar and Jha (Kumar & Jha, 2018b) investigated numerically the cone-shaped vortex finders effect on the cyclone performance. They show that the cyclone performance improved with increasing the cone angle from zero to 50. However, the cone angle has a negative effect on the values of 50 to 100. In another study, They (Kumar & Jha, 2018a) optimized the vortex finder geometry for increasing the cyclone efficiency based on Response Surface Methodology (RSM) and Genetic Algorithms (GA). Their results show that Genetic algorithms solution was better than RSM. Also, divergent or convergent-divergent vortex finder has better performance. Mahmoodabadietal. (Mahmoodabadi, Taherkhorsandi, & Safikhani, 2013) have been optimized a cyclone based on PSO method. In this study, pressure drop and collection efficiency were objectives of optimization. Luciano et al. (Luciano, Silva, Rosa, & Meier, 2018) optimized three cyclones in series for increasing the efficiency and decreasing the pressure drop. The results displayed that the height and the width of the inlet have a significant role in optimization. Lim et al. (Lim, Park, Lee, Zahir, & Yook, 2019) investigated the numerical effect of additional inlets of the cone section on the cyclone separator performance. Results show that additional inlets provide higher flowrate with similar performance. Lee and Yoon (Le & Yoon, 2020) studied the cyclone separator performance for two new designs with four inlets. They changed the location of inlets along the vertical direction for a new design. Results show that both new designs have better performance than the reference cyclone separator with one inlet. Qiang et al. (Qiang, Qinggong, Weiwei, Zilin, & Konghao, 2020) investigated numerically and experimentally performance of a cyclone separator with different vortex finders. New vortex finders had cuts in different locations. Results show that novel vortex finders have improved the efficiency from 0.73 to 76%.

Another inertia-based particle separation equipment is inertial particle separator. Inertial particle separator systems are used for inlet air filtration of the gas turbine engines. Some research has been performed in this field in recent decades (B. Vittal, D. Tipton, 1986; D. Breitman, E. Dueck, 1985; Duffy, 1975; McAnally, 1971). Baron et al. (Barone, Loth, & Snyder, 2014a) studied the flow pattern in an inertial particle separator using the PIV method. They show that the average flow field fits expectations. Also, in another research (Barone, Loth, & Snyder, 2014b), they examined the effect of the inertial particle separator on small particles using Multi-Phase Particle Image Velocimetry. Baron et al. (Barone, Loth, & Snyder, 2017) investigated the effect of particle size on inertial particle separator efficiency. The results show that efficiency was 100% for particle diameters of 120 micrometers. In addition, they show that collection efficiency decreased by particle size reduction. Barone et al. (Barone & Loth, 2015) demonstrated that the design of the Geometry has a significant effect on the efficiency of an inertial particle separator. Baron et al. (Barone, Dominic; Loth, Eric; Snyder, 2018) Studied the two-dimensional flow visualization in an inertial particle separator. Their results indicate a high performance (over 90%) for the inertial particle separator. Collin et al. (Collin M. Goss, 1 Brian J. Connolly, 2019) investigated numerically and experimentally performance of an inertial particle separator using 2D RANS and PIV, respectively. Results show that 2D RANS is a good method for the study of the inertial sand separator performance. Cannolly et.al (Connolly, Brian J.; Loth, Eric; Snyder, Philip H.; Smith, 2019) studied the effect of the geometrical parameters on the inertial sand separator efficiency. PIV method has been used for the evaluation of the cyclone performance. Results show that the hub-side ramp increases the separation efficiency.

Inertial sand separators are employed in gas turbine power plants for the cleaning of the compressor intake air. Geometry and performance of this system are different from other mentioned IPS systems. Regarding the purchase price of this equipment and their electricity consumption, it is substantially paramount to study their performance which has been rarely addressed in previous studies. This study aims to numerically simulate one stage of the inertial sand separator filtration system of Kaveh gas turbine power plant (Qaen, Iran) using Ansys Fluent 16, as well as investigating the collection efficiency for different diameters and densities of dust particles.

2. Introduce of Inertial Sand Separator

To refine and remediate the compressor intake air the gas turbine power plant cycle, the air is

passed through several different filters so that dust particles are removed. In the first step, large objects are removed by a steel filter. Inertial Sand separators (extensively explained in what follows) are placed in the next position and cartridge filters are positioned at the end so that air is fully remediated. Air remediation not only does enhance the efficiency of a gas turbine power plant but also lengthens the lifetime of the turbine and compressor blades. As already posited, one of these filters is the inertial sand separators system. Figure 1 shows schematic of inertial sand separators system. In figure1, number 1 introduces the inertial sand separators and number 2 displays the particle collector. Figure 2 depicts the views of airflow in an inertial sand separator. As shown in figure 2, in an inertial sand separator, air enters the chamber through their inlets and passes through groves embedded in the chamber body. These grooves change the direction of airflow and, in turn, lead the heavy-weight particles (large-grain pollutions) to be unable to simultaneously change direction and they get trapped in the bottom of the chamber. Finally, these particles are blown out of the chamber by fans. Figure 3 shows the schematic of an inertial sand separator. Table 1 determines the dimensions of an inertial sand separator.

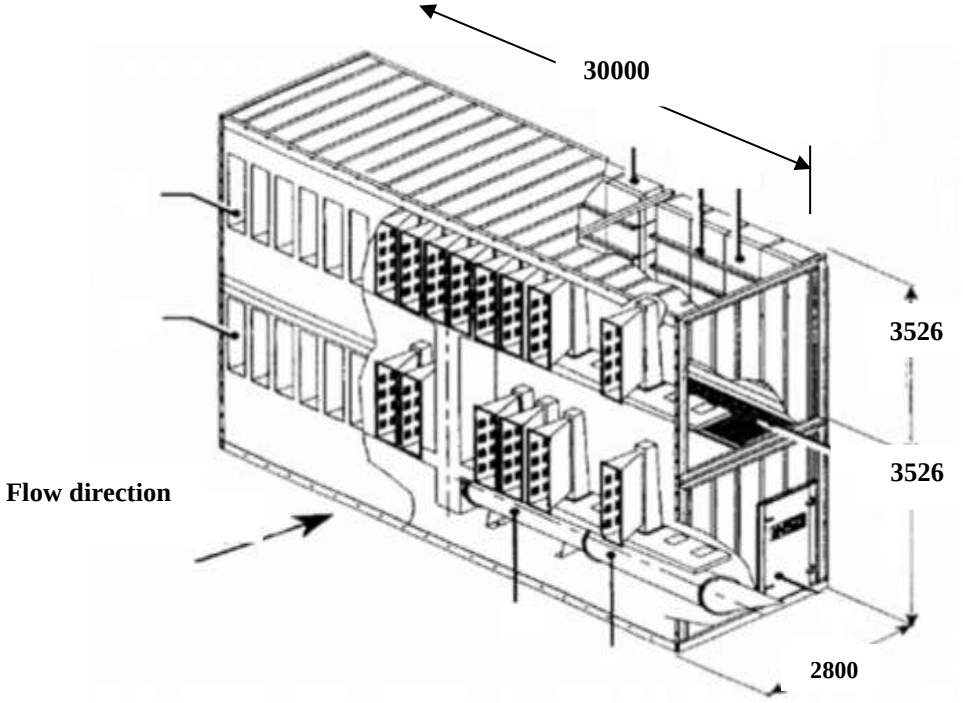

Figure 1. schematic of inertial sand separators system (dimension in mm)

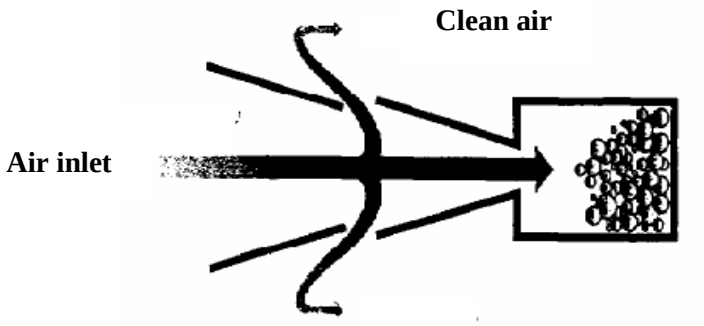

Figure 2. schematic of the air flow in an inertial sand separator

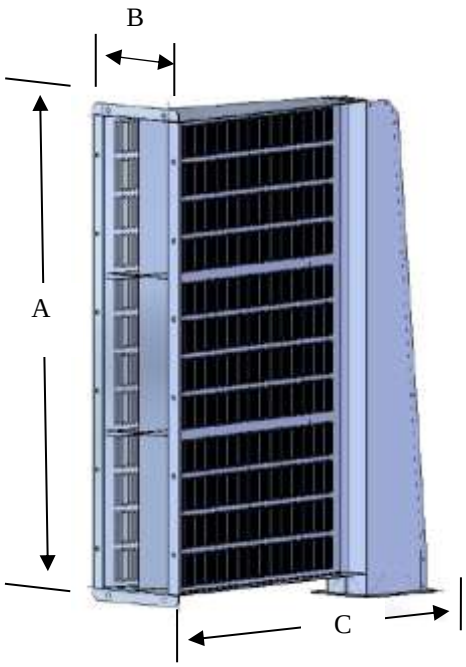

Figure 3. Schematic of an inertial sand separator

Table 1. Dimension of an inertial sand separator

Dimension	Size (mm)
A	**1560**
B	**220**
C	**1150**

3. Problem Geometry, Governing Equations, and Numerical Simulation

The schematic of the inertial sand separators, exhaust channel connected to the fan, and airflow path are shown in figure 4. This geometry is equipped with 30 air triangular inlets that decrease in cross-sectional area along the flow stream as a converging path. There are some grooves on the wall of the inertial sand separators representing the air inlet path towards the compressor. As can be observed in the figure, the airflow travels in the converging path of the inertial sand separators after the entrance and a portion of flow move towards the compressor through the grooves and the other portion rotate within the inertial sand separators and have reverse movements leading to the fall of particles in the channel. As a collector, the channel connected to the inertial sand separators transports the dusty flow towards the fan.

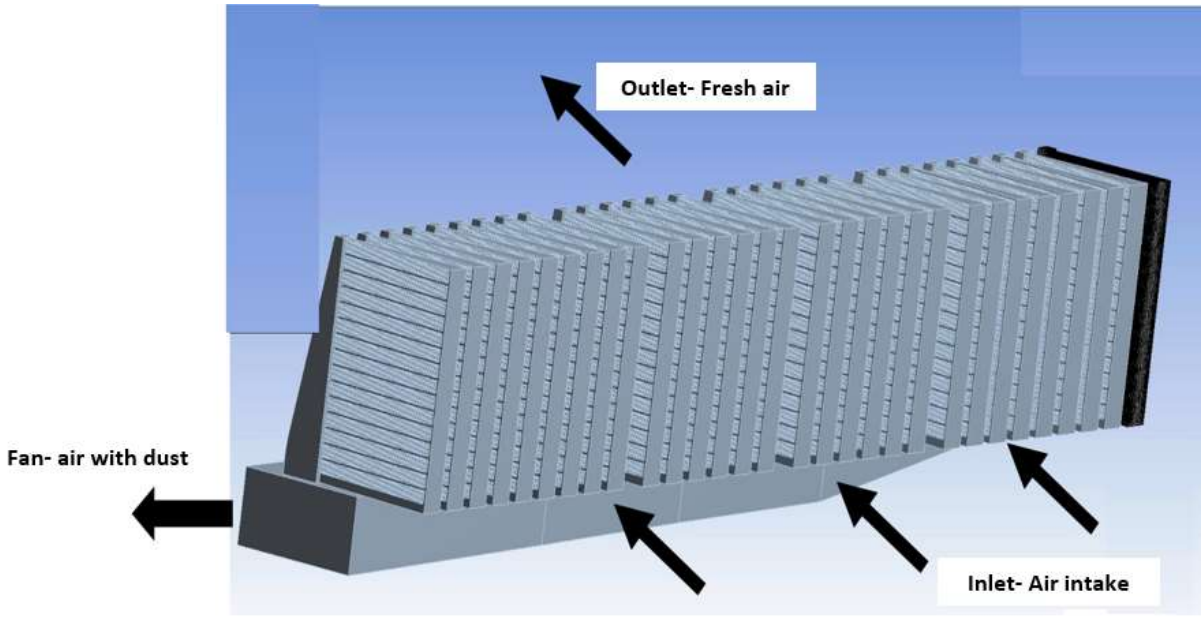

Figure 4. Schematic view of the inertial sand separators

ANSYS 16 software was used for the simulation. Regarding the immense computations, a computational server with 20 processing cores and RAM of 120 GB was used to carry out the calculations. According to the power plant data (*Performance test of Kave combined cycle PP (GT V94.2). (n.d.).*, n.d.), the following assumptions were considered for boundary conditions: inlet condition, atmospheric pressure, fan outlet condition,

known relative negative pressure of 800 Pa, and clean air exiting from the grooves with the known relative negative pressure of 300 Pa. The SIMPLE algorithm was implemented to discretize pressure and momentum terms. Based on the experience, the convergence criterion of equations was selected to be10^{-5}. As the flow is swirling with a high-pressure gradient, the flow regime is assumed turbulence. To model turbulence, the standard $k-\varepsilon$ model was used which is focused on the operations influencing the kinetic turbulent energy. For this model, two transport equations are solved to calculate kinetic energy (k) and turbulence dissipation (ε), as given below(Pope, 2007)

$$\frac{\partial}{\partial t}(\rho k)+\frac{\partial}{\partial x_i}(\rho k u_i) = \frac{\partial}{\partial x_i}\left(\alpha_k \mu_{eff}\frac{\partial k}{\partial x_j}\right) + G_k + G_b - \rho\varepsilon - Y_m \quad (1)$$

$$\frac{\partial}{\partial t}(\rho \varepsilon)+\frac{\partial}{\partial x_i}(\rho \varepsilon u_i) = \frac{\partial}{\partial x_i}\left(\alpha_\varepsilon \mu_{eff}\frac{\partial \varepsilon}{\partial x_j}\right) + C_{1\varepsilon}\frac{\varepsilon}{k}(G_k + C_{3\varepsilon}G_b) - C_{2\varepsilon}\rho\frac{\varepsilon^2}{k} \quad (2)$$

In these equations, constant coefficients are as follows: $\alpha_\varepsilon = 0.72$, $C_\mu = 0.0845$, $\alpha_k = 0.72$, $C_{1\varepsilon} = 1.42$, and $C_{2\varepsilon} = 1.68$ (Pope, 2007).

To calculate the velocity of particles, the following momentum equation has been used (Saeed & Al-Garni, 2007):

$$m_p \frac{du_p}{dt} = F \quad (3)$$

The forces applied to particles include drag and gravity forces, and particles have been assumed to be sphere-shaped. Therefore, this momentum equation would be as follows:

$$\frac{\pi}{6}\rho_P {d_p}^3 \frac{du_p}{dt} = F_D + F_G \quad (4)$$

The drag force is calculated based on the sliding speed between particle and fluid flow, as expressed below:

$$F_D = \frac{1}{2}C_D \rho A_f {u_s}^2 \quad (5)$$

Here, the drag coefficient is calculated from the following relation (Saeed & Al-Garni, 2007):

$$C_D = Max\left[\frac{24}{\mathrm{Re}_p}(1+.15\mathrm{Re}^{0.687}), 0.44\right] \quad (6)$$

And, particle Reynolds number is calculated as follows:

$$\mathrm{Re}_p = \frac{\rho d_p u_s}{\mu} \quad (7)$$

And the net force induced by gravity is calculated as:

$$F_G = \frac{\pi}{6}{d_p}^3(\rho_p - \rho)g \quad (8)$$

The mesh independency is investigated in figure 5. To verification of the results, velocity values in the middle parts of different stages at the inlet of inertial sand separators are shown in figure 3 for different meshes. Based on the figure, the mesh with a total of 13654312 grids is selected as the optimum mesh.

Figures 6 and 7 depict the mesh in thorough and magnified views, respectively. This mesh has been finer close to the grooves due to the presence of severe velocity gradients so that the results would be more accurate.

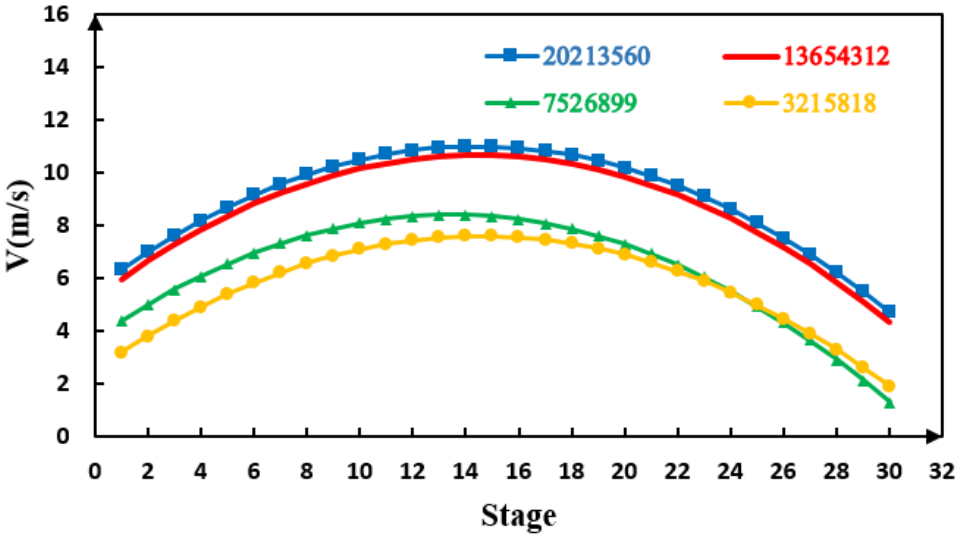

Figure 5. Comparison of velocity values for different meshes

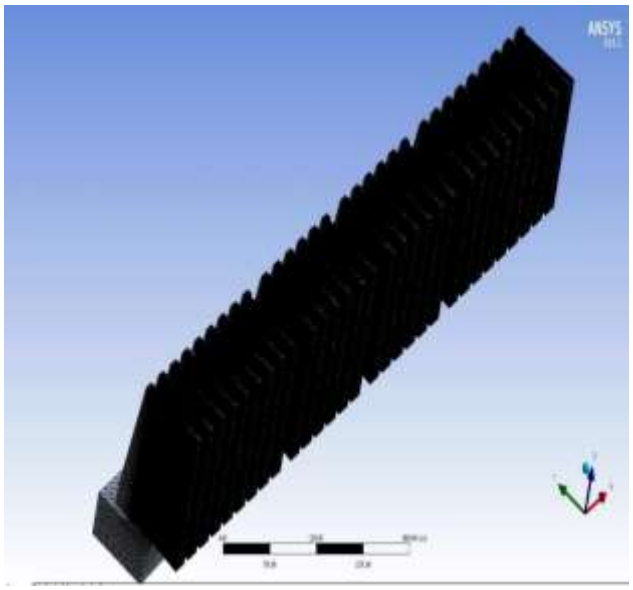

Figure 6. Thorough view of the meshed geometry

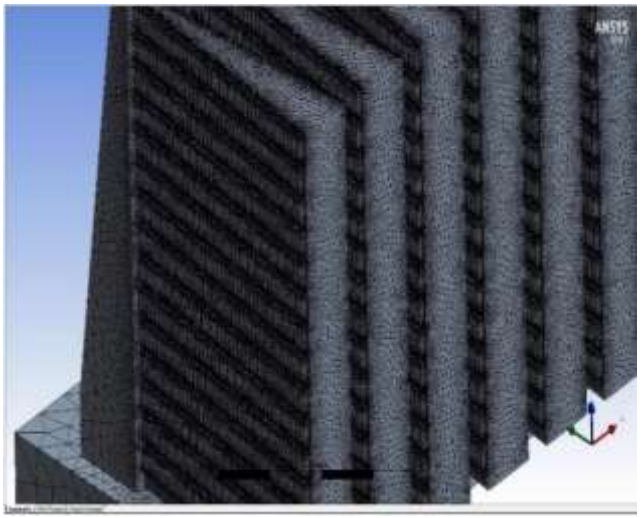

Figure 7. Magnified view of the meshed geometry

4. Results

To validate the results, figure 8 compares the velocity values obtained from numerical solution and measurements in a gas turbine power plant in middle parts of different stages (*Performance test of Kave combined cycle PP (GT V94.2). (n.d.).*, n.d.) at the inlet of inertial sand separators. As can be observed, the numerical results have a good agreement with experimental results. Furthermore, due to the maximum suction in the middle region of the compressor, the velocity at the middle stages has reached its maximum. The symmetry of velocity values relative to the center is another proof of consistency between numerical and experimental results.

Figure 9 shows the results of pressure distribution in the entire inertial sand separators and channel. As can be seen, the suction has increased gradually across the channel towards the fan at the final stages. Moreover, the fan suction has affected the channel merely from its first stages to its middle. Based on the pressure values, the fan suction cannot affect the first 9 stages of the channel. Also, it can be observed that the suction is expected to increase from the top to the bottom of the channel in the vertical direction that this increase is drastically high at the final stages close to the fan.

In figure 10, the particle trajectory is depicted within the entire sand separators and channel. According to the figure, many particles exit from the grooves, and only a limited number of particles are sucked by the fan. For the stages close to the fan, the effect of the fan on the suction of particles is more dominant, i.e. the fan practically does not affect the suction of particles at stage 9 and preceding stages.

Figure 11 depicts the velocity values in the entire inertial sand separators and channel. As can be observed, at the end of the inlet channel in the vicinity of the fan, the velocity reaches its maximum due to the maximum suction. Furthermore, the velocity at the final stages of the channel is dramatically higher than that at the primary stages. In other words, it can be concluded the fan suction hasn't affected the first 9 stages of the channel.

Figure 12 depicts the velocity vectors. As can be observed, the magnitude of velocity vectors increases across the fan suction and dramatically varies between the primary and final stages such that the fan effect is negligible on the velocity of the primary stages of the channel. Based on the figure, velocity magnitude changes between zero to 20 m/s in the stages and channel.

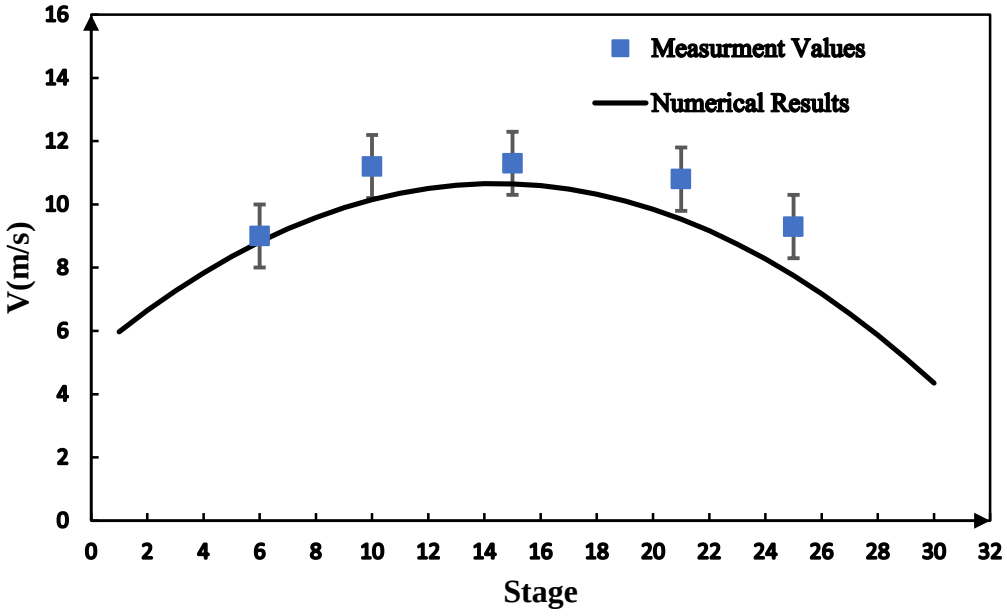

Figure 8. Comparison of velocity values obtained from the numerical solution and measurements (*Performance test of Kave combined cycle PP (GT V94.2). (n.d.).*, n.d.)

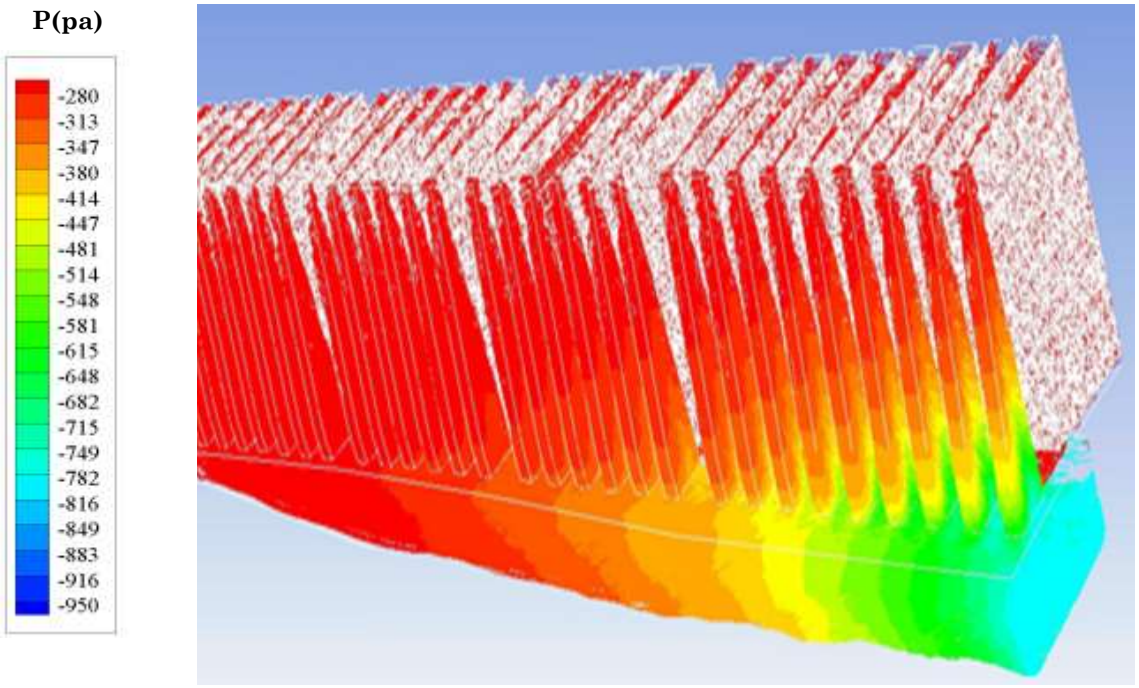

Figure 9. Pressure distribution in the entire inertial sand separators and channel

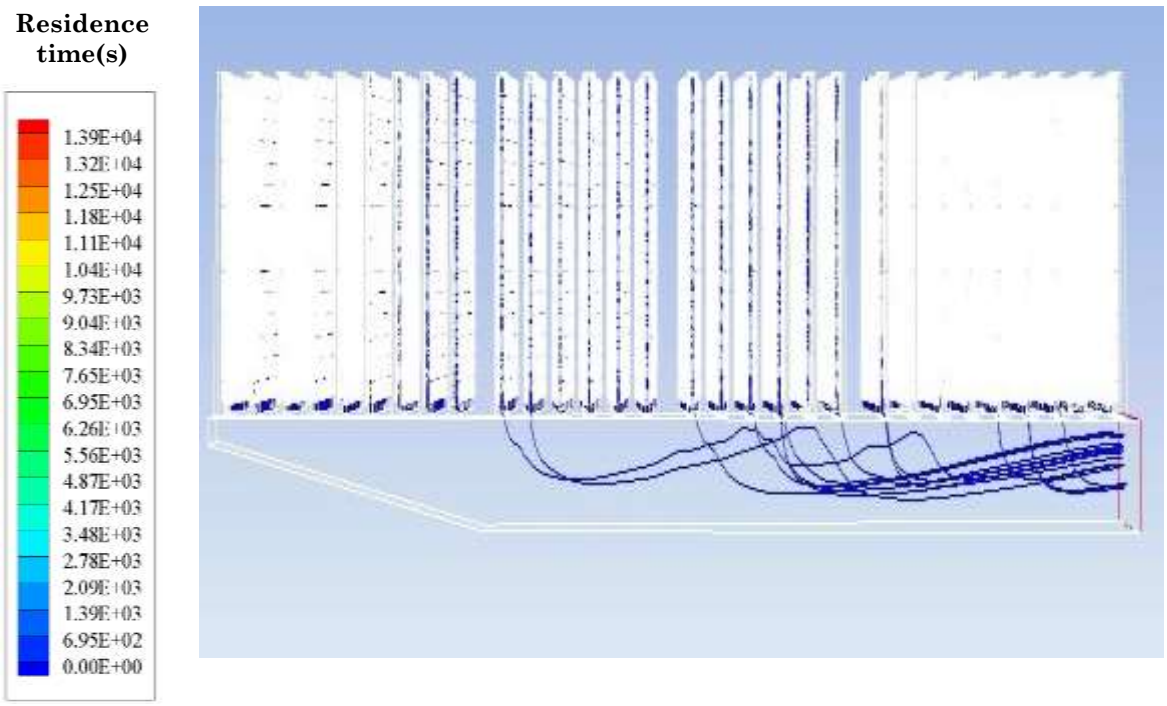

Figure 10. The trajectory of particles in the entire inertial sand separators and channel

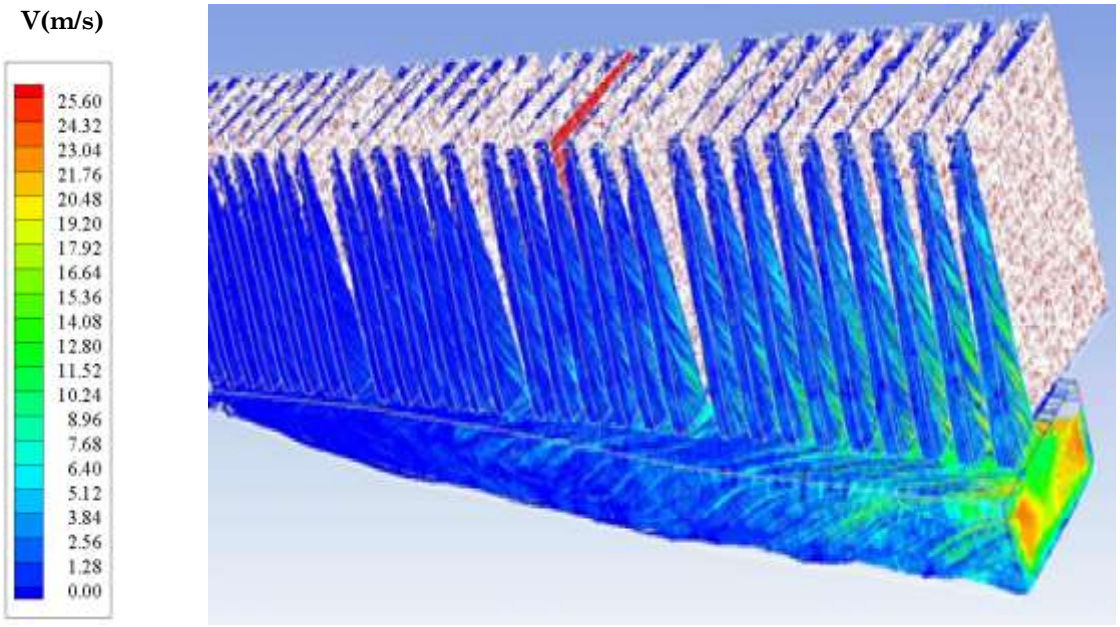

Figure 11. Velocity magnitudes in the entire inertial sand separators and channel

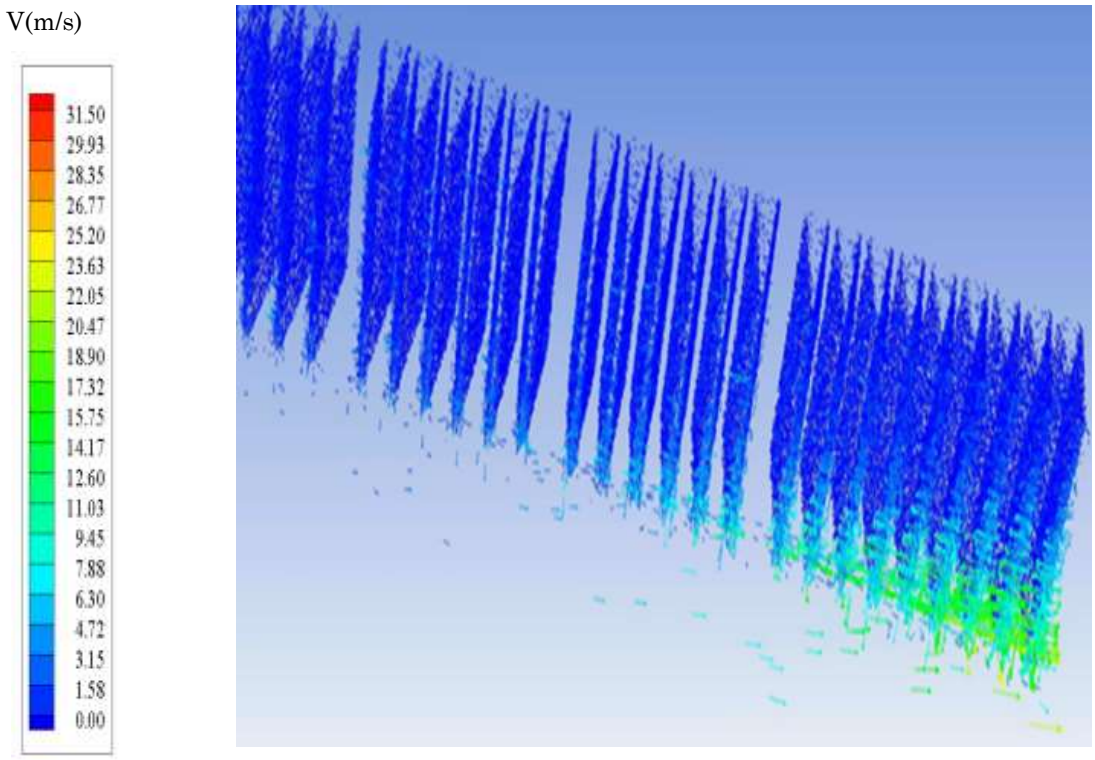

Figure 12. Velocity vectors the entire inertial sand separators and channel

Figure 13 investigates the inertial sand separators' performance for different particle diameters. The diagram depicts the number of fan exiting particles versus the diameter of particles with a density of $1000 kg/m^3$. The results have been examined for a total of 4959 particles with four different diameters. As can be observed, increasing the diameter of particles, the number of fan exiting particles is reduced. This could be attributed to the fact that the drag forces exerted on the particle increase as the particle is enlarged in diameter where the fan suction is not sufficient to overcome the drag force of large particles. According to the number of entering particles and figure 13, the maximum collection efficiency of the inertial sand separators system is around 0.5%, implying that this system is inefficient and not cost-effective.

Figure 14 depicts the number of fan exiting particles with a diameter of $0.1\mu m$ and different densities. It can be observed that as the density of particles increases, the number of fan exiting particles is augmented as well. This is because more particles are trapped in the channel (the fan gets a higher chance for the suction of particles) once the density of particles rises (i.e. increasing the weight of particles). Regarding the number of entering particles and figure 14, the maximum collection efficiency of the inertial sand separators system is about 0.5%, implying that this system is inefficient and not cost-effective.

Based on the above results, the system fans can be removed. There are 20 fans for the inertial sand separators system in Shahid Kave power plant. As the power of each fan is 18 kW, the Elimination of 20 fans could reduce the energy consumption of the gas power plant around 360 kW.

Also, the new fans could be substituted for problem-solving. Figure15 shows the flowchart for the process of problem solving. Based on the flowchart, by increasing the fan suction gradually and then checking the collection efficiency, new appropriate fans can be substituted for problem-solving.

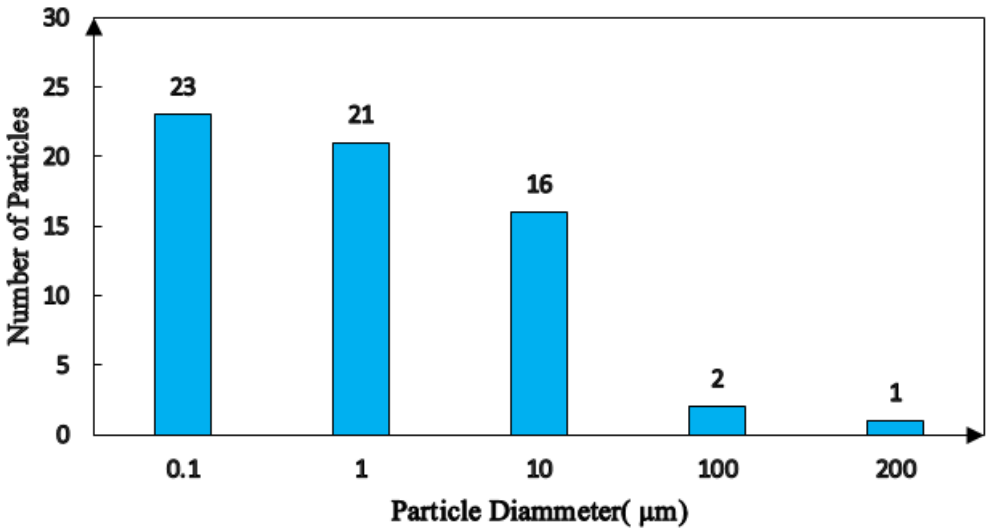

Figure 13. The total number of fan exiting particles for different diameters of particles

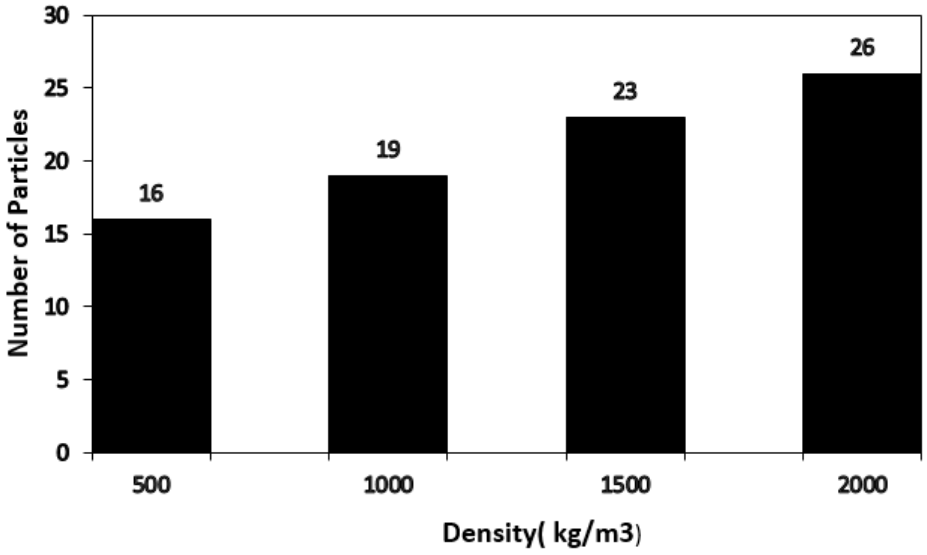

Figure 14. The total number of fan exiting particles for different densities of particles

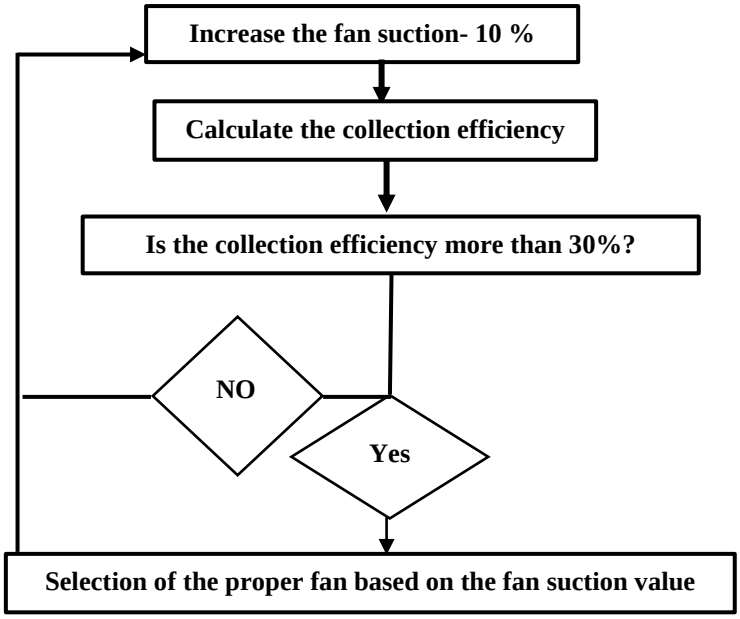

Figure 15. Flowchart of problem-solving

5. Conclusion

In the present study, the numerical simulation of the inertial sand separators system of Kaveh power plant (Qaen, Iran) was carried out by ANSYS Fluent 16 software. Furthermore, the velocity and pressure fields have been studied and the effect of diameter and density of particles on the collection efficiency of inertial sand separators system has been examined as well. Based on the obtained results, the following are presented:

1. The suction of the fan hasn't affected the first 9 primary stages of the channel.
2. The collection efficiency of the inertial sand separators system was reduced by increasing the particle diameter.
3. The collection efficiency of the inertial sand separators system was improved by increasing the particle density.
4. The collection efficiency of the inertial sand separators system was substantially low, i.e. lower than 1% for all states.
5. The elimination of the system fans could reduce the energy consumption of the gas power plant around 360 kW.

Acknowledgement

This research would not have been possible without the financial support Kave combined cycle power plant. We thank our colleagues from this company who provided insight and expertise that greatly assisted the research.

Nomenclature

A_f	Effective particle cross section(m^2)
C_D	Drag coefficient
d_p	Particle diameter (m)
F	Force (N)
F_D	Drag force (N)
F_G	Net force due to gravity (N)
G_k	Generated turbulent energy due to the variations in mean velocity (kg/m. s^3)
G_b	Generated turbulent energy due to the buoyancy force (kg/m. s^3)
g	Gravitational acceleration constant (m/s^2)
k	Turbulent kinetic energy (m^2/s^2)
m_p	Particle mass (kg)
u_i	Fluid velocity for ith component (m/s)
u_p	Particle velocity (m/s)
u_s	Slip velocity between the fluid and the particle (m/s)
Re_p	Reynolds number based on particle
t	Time(s)
x_i	ith coordinate direction
x_j	jth coordinate direction
Y_m	Contribution of expansion fluctuations to the compressible turbulence with respect to the total rate of turbulence dissipation

Greek Symbols

α_k	Thermal diffusivity for turbulent kinetic energy (m^2/s)
α_ε	Thermal diffusivity for turbulent dissipation rate (m^2/s)
ε	Turbulence dissipation rate (m^2/s^3)
ρ	Fluid density (kg/m^3)
ρ_p	Particle density (kg/m^3)
μ	Viscosity (kg/m.s)
μ_{eff}	Effective viscosity (kg/m.s)

References

Amini, H., Lee, W., & Di Carlo, D. (2014). Inertial microfluidic physics. *Lab on a Chip*, *14*(15), 2739–2761. https://doi.org/ 10.1039/c4lc00128a.

B. Vittal, D. Tipton, W. B. (1986). Development of an advanced vanesless inlet particle separator for helicopter engines. *Journal of Propulsion*, *5*(2), 438–444.

Barone, Dominic; Loth, Eric; Snyder, P. H. (2018). Flow Field and Efficiency of a Two-Dimensional Inertial Particle Separator. *Journal of the American Helicopter Society*, *63*(1), 1–9. https://doi.org/10.2514/6.2019-4340.

Barone, D., & Loth, E. (2015). *Efficiency of an Inertial Particle Separator*. *31*(4). https://doi.org/10.2514/1.B35276.

Barone, D., Loth, E., & Snyder, P. (2014a). Fluid Dynamics of an Inertial Particle Separator. *52nd Aerospace Sciences Meeting*. National Harbor, Maryland.

Barone, D., Loth, E., & Snyder, P. (2017). Influence of particle size on inertial particle separator efficiency. *Powder Technology*, *318*, 177–185. https://doi.org/10.1016/j.powtec.2017.04.044.

Barone, D., Loth, E., & Snyder, P. H. (2014b). PARTICLE DYNAMICS OF A 2-D INERTIAL PARTICLE SEPARATOR. *Proceedings of ASME Turbo Expo 2014: Turbine Technical Conference and Exposition*. Düsseldorf, Germany.

Collin M. Goss, 1 Brian J. Connolly, 2 and Eric Loth3. (2019). Performance, 2D Scaling and Axisymmetric Effects on Inertial Particle Separator. *AIAA Propulsion and Energy 2019 Forum*. https://doi.org/https://doi.org/10.2514/6.2019-4340.

Connolly, Brian J.; Loth, Eric; Snyder, Philip H.; Smith, C. F. (2019). Influence of Scavenge Leg Geometry on Inertial Particle Separator Performance. *Journal of the American Helicopter Society*, *64*(3), 1–12.

D. Breitman, E. Dueck, W. H. (1985). Analysis of a split-flow inertial particle separator by finite elements,. *J. Aircr*, *22*(2), 135–140.

Duffy, R. J. (1975). Integral engine inlet particle separator . Design Guide. In *Tech.Rep. AD-A015 064, General Electric Company*.

Khazaee, I. (2017). Numerical investigation of the effect of number and shape of inlet of cyclone and particle size on particle separation. *Heat and Mass Transfer/Waerme- Und Stoffuebertragung*, *53*(6), 2009–2016. https://doi.org/10.1007/s00231-016-1957-4.

Kumar, V., & Jha, K. (2018a). Multi-Objective Shape Optimization of Vortex Finders in Cyclone Separators Using Response Surface Methodology and Genetic Algorithms. *Separation and Purification Technology*. https://doi.org/10.1016/j.seppur.2018.12.083.

Kumar, V., & Jha, K. (2018b). Numerical investigations of the cone-shaped vortex finders on the performance of cyclone separators. *Journal of Mechanical Science and Technology*, *32*(11), 5293–5303. https://doi.org/10.1007/s12206-018-1028-5.

Le, D. K., & Yoon, J. Y. (2020). Numerical investigation on the performance and flow pattern of two novel innovative designs of four-inlet cyclone separator. *Chemical Engineering & Processing: Process Intensification*, *150*. https://doi.org/10.1016/j.cep.2020.107867.

Lim, J., Park, S., Lee, H., Zahir, M. Z., & Yook, S. (2019). Performance evaluation of a tangential cyclone separator with additional inlets on the cone section. *Powder Technology*. https://doi.org/10.1016/j.powtec.2019.09.056.

Luciano, R. D., Silva, B. L., Rosa, L. M., & Meier, H. F. (2018). Multi-objective optimization of cyclone separators in series based on computational fluid dynamics. *Powder Technology*, *325*, 452–466. https://doi.org/10.1016/j.powtec.2017.11.043.

Mahmoodabadi, M. J., Taherkhorsandi, M., & Safikhani, H. (2013). Modeling and Hybrid Pareto Optimization of Cyclone Separators Using Group Method of Data Handling (GMDH) and Particle Swarm Optimization (PSO). *International Journal of Engineering*, *26*(9), 1089–1102. https://doi.org/10.5829/idosi.ije.2013.26.09c.15.

McAnally, W. J. (1971). Investigation of feasibility of integral gas turbine

engine solid particle inlet separators. *Proceedings of the 10th Annual National Conference on Environmental Effects on Aircraft and Propulsion Systems*, (1), 25.

Performance test of Kave combined cycle PP (GT V94.2). (n.d.). (n.d.).

Pope, B. S. (2007). *Turbulence Flows*. United states of America, New York: Cambridge University Press.

Qiang, L., Qinggong, W., Weiwei, X., Zilin, Z., & Konghao, Z. (2020). Experimental and computational analysis of a cyclone separator with a novel vortex finder. *Powder Technology*, *360*, 398–410. https://doi.org/10.1016/j.powtec.2019.10.073.

Saeed, F., & Al-Garni, A. Z. (2007). Analysis Method for Inertial Particle Separator. *JOURNAL OF AIRCRAFT*.

Safikhani, H. (2016). Modeling and multi-objective Pareto optimization of new cyclone separators using CFD , ANNs and NSGA II algorithm. *Advanced Powder Technology*. https://doi.org/10.1016/j.apt.2016.08.017.